Polymer Microstructures. Modification and Characterisation by Fluid Sorption

Séverine A.E. Boyer, Mohamed Baba, Jean-Marie Nedelec, Jean-Pierre E. Grolier

Polymer Microstructures. Modification and Characterisation by Fluid Sorption [1]

S. A. E. Boyer[2,3,4], M. Baba[2,] J-M. Nedelec[5] and J-P. E. Grolier[2,6]

Polymer micro-organisation can be modified by combination of the three constraints, thermal, hydrostatic and fluid sorption. In selecting the fluid's nature, chemically active or inert, and its physical state, liquid or supercritical, new "materials" can be generated. In addition, the interplay of temperature and pressure allows tailoring the obtained material structure for specific applications. Several complementary techniques have been developed to modify, analyze and characterize the end products: scanning transitiometry, vibrating wire (VW)-PVT coupling, thermoporosimetry, temperature modulated DSC (TMDSC), sorptometry. The great variety of possible applications in materials science is illustrated with different polymers which can produce materials from soft gel to rigid foams when submitted to fluid sorption, typical fluids being methane, or a simple gas (CO_2 or N_2).
Absorption of an appropriate fluid in a cross linked polymer leads to a swelling phenomenon. Thermoporosimetry is a calorimetric technique developed to measure the shift by confinement of thermal transition temperatures of the swelling fluids, which can be currently used solvents or mercury. Application of thermoporosimetry to a swollen cross linked polymer allows to calculate the mesh size distribution and to evaluate the degree of reticulation of the polymer. The same technique can be applied to characterise the pore size distribution in a foamed polymer.

KEY WORDS: scanning transitiometry, vibrating wire weight sensor, thermoporosimetry, temperature modulated DSC, polymer foam, mesh size distribution, pore size distribution

[1] Paper presented at Thermo International 2006, July 30 – August 4, 2006, Boulder, Colorado, USA.
[2] Laboratory of Thermodynamics of Solutions and Polymers, Blaise Pascal University, 24, Avenue des Landais, 63177 Aubière, France.
[3] Department of applied Chemistry, Graduate School of engineering, Tokyo Metropolitan University, Hachiouji, Tokyo, Japan.
[4] Present address: Centre de Mise en Forme des Matériaux (CEMEF), Ecole Nationale Supérieure des Mines de Paris, 06904 Sophia Antipolis, France.
[5] Laboratoire des Matériaux Inorganiques CNRS UMR 6002, Université Blaise Pascal, Clermont-Ferrand 2 & Ecole Nationale Supérieure de Chimie de Clermont-Ferrand, 24, Avenue des Landais, 63177 Aubière, France
[6] To whom correspondence should be addressed. E-mail: j-pierre.grolier@univ-bpclermont.fr

1. INTRODUCTION

Selection of materials is usually made according to their thermophysical properties and their structural characteristics. In numerous industrial applications, in nano-science at large, making use of advanced nano-technologies, polymers are playing a major ~~central~~ role. Due to their intimate native structures to the many modified structures ??? polymers offer a large spectrum of useful all purpose materials. Among possible tailored polymer structures most of them are obtained by modifying the polymer micro-organizations through foaming processes. The polymer foaming sector is certainly one of the most active branches of the industrial activity in materials science. Efficient foaming is developed by using selected blowing agents. As a result of the negative impact on the environment of most of the blowing agents traditionally employed up to now, an international regulation has imposed a ban on all chlorofluorohydrocarbons types blowing agents. Replacement agents, including simple gases like CO_2 or N_2, are currently proposed and experienced [1]. There from ongoing active researches are focused on gas/polymer interactions in terms of energy of interaction, solubility as well as polymer swelling under gas sorption. As a matter of fact, the micro-organization of polymers can be modified by combination of three constraints, thermal, hydrostatic and fluid sorption. In selecting the fluid's nature, chemically active or inert, and its physical state, liquid or supercritical, new "materials" can be generated. Furthermore, the interplay of temperature and pressure allows obtaining material structures to demand for specific applications. In this context, several complementary techniques have been developed to analyze, characterize and modify the polymers'organization: scanning transitiometry [2], vibrating wire (VW)-PVT coupling [3], thermoporosimetry [4] and temperature modulated DSC (TMDSC) [5]. In what follows, the different techniques are shortly described and selected examples are used to illustrate their pertinent contribution.

2. SCANNNG TRANSITIOMETRY

The use of state variables (*p, V and T*) in scanning calorimetric measurements has lead [2, 3] from P V T- calorimetry to the now well established scanning transitiometry technique [4]. With this technique the simultaneous determination of thermal and mechanical responses of the investigated system, pertubated by a variation of an independent thermodynamic variable while the other independent variable is kept automatically constant, allows the determination of thermodynamic derivatives over extended ranges of pressure and temperature, impossible to obtain by other known techniques. Four thermodynamic situations are thus possible to realize in the instruments based on such technique, namely, pVT-controlled scanning calorimeters or simply scanning transitiometers, since they are particularly adapted to investigate transitions by scanning one the three thermodynamic variables. The four possible thermodynamic situations are obtained by simultaneous recording of both heat flow (thermal output) and the change of the dependable variable (mechanical output). Then, making use of the respective related Maxwell relations one readily obtains the main thermophysical properties as follows: *a)* scanning pressure under isothermal conditions yields the isobaric thermal expansivity α_P and the isothermal compressibility κ_T as functions of pressure at a given temperature; *b)* scanning volume under isothermal conditions yields the isochoric thermal pressure coefficient β_V and the isothermal compressibility κ_T as functions of volume at a given temperature; *c)* scanning temperature under isobaric conditions yields the isobaric heat capacity C_P and the isobaric thermal expansivity α_P; *d)* scanning temperature under isochoric conditions yields the isochoric heat capacity C_V and the isochoric thermal pressure coefficient β_V.

A detailed description of a basic scanning transitiometer (from BGR TECH, Warsaw, Poland) used in the present applications to polymers is given elsewhere [5]. It consists of a calorimeter equipped with high-pressure vessels, a PVT system, and a LabVIEW based virtual instrument (VI) software. Two cylindrical calorimetric detectors (ext. diameter 17 mm, length 80 mm) made from 622 thermocouples chromel-alumel each are mounted differentially and connected to a nanovolt amplifier. The calorimetric detectors are placed in a calorimetric metallic block, the temperature of which is directly controlled with an entirely digital feedback loop of 22-bit resolution (~10^{-4} K), being part of the transitiometer software. The calorimetric block is surrounded by a heating-cooling shield connected to an ultracryostat

(Unistat 385 from Huber, Germany) and the temperature difference between the block and the heating-cooling shield is set constant (5, 10, 20 or 30 K) as controlled by an analogue additional controller. The whole assembly is placed in a thermal insulation enclosed in a stainless steel body and placed on a stand, which permits to move the calorimeter up and down over the calorimetric vessels. The actual operating ranges of scanning transitiometry are respectively 173 K < T < 673 K and 0.1 MPa < p < 200 MPa (or 400 MPa).

Figure 1 here

According to its basic principle a scanning transitiometer can then be operated in different scanning situations. In particular two main scanning situations, as described in Fig. 1, have been used: pressure-controlled scanning transitiometry (PCST) and temperature-controlled scanning transitiometry (TCST). In addition, the differential mounting of the calorimetric detector permits to measure the differential heat flux, between the reference and the measuring cells, resulting from the physicochemical effects occurring in the investigated systems/phenomena. The advantage of PCST is well illustrated by the study of gas/polymer systems, in particular during sorption (compression by gas-pressurizing fluid)/desorption (by decompression of gas-pressuring fluid) pressure scans. Taking advantage of the respective role of the measuring and reference cells, two modes have been preferably used, as shown Fig.2 (a et b), the thermal differential comparative in which two different polymers can be directly compared and the thermal differential in which a polymer sample is characterized vs an inert reference (steel for example). For each thermal mode, the measured heat rate with polymer was corrected for the heat effects produced by pressurization/depressurization of the hydraulic fluid (expansibility) and the volume sample (asymmetry of the cells). The thermal differential comparative mode was chosen to directly compare the difference in behavior of two polymers submitted simultaneously to the sorption/desorption of the same gas under the same T and P conditions. For this, samples of identical size and shape of two polymers, medium density polyethylene (MDPE) and poly(vinylidene fluoride) (PVDF) were placed in the two cells both connected to the gas line. Isothermal pressure scans were performed using CO_2 as pressure transmitting fluid. Measurements were taken on polymers in the solid state, *i.e.* between glass and melting transitions temperatures, at different temperatures between 353 and 403 K and at each temperature pressure was scanned up to 100 MPa. The calorimetric signal, that is the comparative {(MDPE-PVDF)/CO_2} differential heat flux, is then proportional to the thermal effect due to the difference of the {polymer/gas} interactions

between the two polymers. Interestingly, below 40 MPa, the calorimetric signal dQ {(MDPE – PVDF)/CO_2}/dP < 0} is endothermic thus PVDF exhibits larger interactions with CO_2 than MPDE. Above 40 MPa the reverse situation is observed, the calorimetric signal dQ {(MDPE – PVDF)/CO_2}/dP > 0} is exothermic showing that MDPE exhibits larger interactions with CO_2 [6].

Figure 2 here

The simple thermal differential mode, as shown Fig.2 (c), where the differential heat flux is measured between the measuring cell containing a polymer sample and the reference cell empty (and not connected to the pressure line) acting only as a thermal reference was used in the temperature-controlled scanning transitiometry (TCST) situation. Typically, TCST was chosen to investigate transitions and modifications of polymers submitted to isobaric temperature scans. For example, measurements were taken on polymer samples in cooling or heating between 223 and 473 K at different pressures up to 100 MPa. Under such possible P-T conditions melting/crystallization and glass transitions can be fully characterized. The hydraulic fluid can either be a neutral fluid like mercury or a simple gas like carbon dioxide, nitrogen or methane. In this context, several studies have been successfully conducted; namely: modification of polystyrene glass transition high pressure methane [7], isobaric thermal expansion of polymers (MDPE, PVDF) in absence or in presence of solubilized gases (CO_2, N_2) [1, 8]. Another advantage of TCST is certainly the possibility, through the rigorous thermodynamic control of the process, to foam polymers. The foam structure (type, size, polydispersity of microcavities) is monitored by controlling both T and P and also the nature of the pressurizing fluid (actually the hydraulic fluid itself) [9]. Regarding nanoscale self-assembled molecular organization in liquid crystalline type amphiphilic diblock copolymers, the use of TCST is well described [6, 10, 11] by the systematic investigation of PEO_m-*b*-$PMA(Az)_n$ type polymers (with m and n degrees of polymerization) containing hydrophilic polyethylene oxide (PEO) and hydrophobic azophenyl (PMA(Az)) moieties. Isobaric scans over the isotropic transition of PEO_{114}-b-$PMA(Az)_{20}$ using either mercury or supercritical CO_2 as pressurizing fluids allowed to demonstrate that “inert” mercury and “chemically active” CO_2 have quite opposite effect on the Clapeyron slope of this transition. That is a lowering of the transition temperature T_{iso} and a concomitant significant decrease of the transition entropy ΔS_{iso} showing that CO_2 sorption into the polymer is facilitated; therefore the molecular self organization at the interface polymer/liquid crystal becomes much easier to

yield nano-scale ordered structure, that is PEO cylinders organized in an hexagonal structure into the liquid crystal domain (see schematic illustration Fig. 3), as confirmed by atomic force microscopy analysis [10].

Figure 3 here

3. VIBRATING WIRE – PVT COUPLING

Processing of polymer foams is easily controlled when using blowing agents acting chemically to lower the glass transition (plasticization effect) and physically to promote the foaming process (nucleation effect). As a matter of fact, tailoring of foam structures, that is to say adjusting the type of cells, their sizes and shapes, is possible through a quantitative evaluation of the amount of gas, very often in supercritical state, absorbed in the polymer and also through a fine tuning of both temperature and pressure during processing (usually extrusion-expansion). When dealing with gas sorption in porous materials [12], that is investigating gas sorption/desorption phenomena depending on the pores distribution, again the quantitative evaluation of the amount of gas involved is before all necessary. A double technique has been developed to meet such requirements. This new concept [13] combines two techniques, a vibrating wire (VW)-sensor and a pressure decay PVT technique. The VW-sensor acts as a force sensor to weigh the material sample during sorption while concomitantly the PVT technique allows to quantitatively estimating the corresponding number of moles of gas absorbed. In the case of a polymer, the buoyancy force exerted by the pressurized fluid on the polymer depends on the swollen volume, ΔV_{pol}, of the polymer due to the gas sorption. The VW-sensor consists essentially of a high pressure cell in which the polymer sample is placed in a holder suspended by a thin tungsten wire (diameter 25 μm, length 30m) in such a way that the wire is positioned in the middle of a high magnetic field generated by a square magnet placed across the high pressure cell. Through appropriate electric circuitry and electronic control the tungsten wire is activated to vibrate. The period of vibration which can be accurately measured is directly related to the mass of the suspended sample. The pressure decay PVT-method allows calculating the number of moles, n_{sol}, of gas [which is initially kept in a high-pressure calibrated cell] absorbed in the polymer, from the measurement of pressure at its initial value p_i when the gas enters the measuring cell and its

final value p_f after the gas-polymer system has returned to thermodynamic equilibrium. The combined VW-PVT apparatus is designed to measure sorption of the gas and the concomitant volume change of the polymer at pressures up to 100 MPa from room temperature to 473 K. The experimental method consists in a series of successive transfers of the gas by connecting the calibrated cell to the equilibrium cell which contains the polymer. The initial, p_i, and final, p_f, pressures are recorded between each transfer. The detailed methodology and the revisited iterative calculation to simultaneously calculate the solubility together with the volume change of the polymer due to sorption [14,15] are using two rigorous working equations.

The working equation (1) for the PVT-technique gives the amount of gas entering the polymer sample during the first transfer once equilibration is attained

$$m_{sol} = \frac{M_g}{R\,T_f}\frac{p_f}{Z_f}\Delta V_{pol} + \frac{M_g}{R}\left[\frac{p_i}{Z_i T_i}V_3 - \frac{p_f}{Z_f\,T_f}\left(V_2 + V_3 - V_{pol}\right)\right] \tag{1}$$

The term m_{sol} is the mass of gas dissolved in the polymer, M_g is the molar mass of the dissolved gas, Z_i with Z_f are the compression factors of the gas entering the polymer respectively at the initial (index $_i$) and final (equilibrium sorption, index $_f$) conditions. Volume of the degassed polymer and the volume change due to sorption are represented by V_{pol} and ΔV_{pol} respectively. And the total amount of gas absorbed by the polymer after completion of the successive transfers is given by equation (2)

$$\Delta m_{sol}^{(k)} = \frac{M_g}{R}\frac{p_f^{(k)}\,\Delta V_{pol}^{(k)}}{Z_f^{(k)}\,T_f^{(k)}} + \frac{M_g}{R}\left[\frac{p_i^{(k)}V_3}{Z_i^{(k)}T_i^{(k)}} + \frac{p_f^{(k-1)}\left(V_2 - V_p - \Delta V_{pol}^{(k-1)}\right)}{Z_f^{(k-1)}T_f{}^{(k-1)}} - \frac{p_f^{(k)}\left(V_2 + V_3 - V_{pol}\right)}{Z_f^{(k)}T_f{}^{(k)}}\right] \tag{2}$$

where $\Delta m_{sol}^{(k)}$ is the increment in dissolved gas mass resulting from the transfer k and $\Delta V_{pol}^{(k)}$ is the change in volume after transfer k.

The working equation (3) for the vibrating-wire sensor VW relates the mass, m_{sol}, of gas absorbed in the polymer to the change in volume, ΔV_{pol}, of the polymer. The natural angular frequency of the wire, through which the polymer sample holder is suspended, depends on the amount of gas absorbed. The physical characteristics of the wire are accounted for in equation (3) as:

$$m_{sol} = \rho\,\Delta V_{pol} + \left[\left(\omega_B^2 - \omega_0^2\right)\frac{4\,L^2\,R^2\,\rho_S}{\pi\,g} + \rho\left(V_C + V_{pol}\right)\right] \tag{3}$$

The terms ω_0 with ω_B represent the natural (angular) frequencies of the wire in vacuum and under pressure respectively, V_C the volume of the container. The symbols L, R and ρs are respectively the length, the radius and the density of the wire.

A common term appears in both equation (2) and equation (3), the density, ρ, of the gas

$$\rho_{gas} = \frac{M_g}{R\,T}\,\frac{p_f}{Z_f} \tag{4}$$

Then equation (3) can be written

$$\Delta m_{sol}^{(k)} = \rho_{gas}\ \Delta V_{pol} + d \tag{5}$$

The term d represents the apparent concentration of gas in the polymer, i.e. when the change in volume, ΔV_{pol}, is zero. However, despite the different terms appearing in the two working equations (2) and (3), these two equations can be both expressed by the same reduced equation (5) having the slope given by equation (4). The vibrating-wire sensor VW is described with rigorous models yielding a working equation in which all parameters have a physical meaning: ω_0 and ω_B the natural frequencies [Hz], V_C [m^3], L [m], R [m] and ρs [kg m^{-3}] of the wire. The pressure decay technique requires Z, M_g [g mol^{-1}] for the gas and the volumes of the cells [m^3]. The volume of the polymer sample, V_{pol}, with its associated change, ΔV_{pol}, and the total mass of dissolved gas, m_{sol}, are the only unknown terms.

It appears that the vibrating-wire sensor technique is more precise than the PVT -technique since there are no cumulative errors like in the case of the PVT -method, when the successive transfers are performed during an isothermal sorption. The technique does not require extensive calibrations. Essentially, uncertainties come from the experimentally measured resonance frequencies. Errors are reduced with the new data acquisition permitting the simultaneous recording of the phase with the frequency: effectively, the phase angle is better suited than the amplitude to detect the natural resonant frequency (and also the half-width) [15]. The main source of uncertainty affecting the evaluation of the gas concentration data comes from the term of equation (5) which contains the density of the gas and the change in volume of the polymer. At this stage, it was then necessary to elaborate a new procedure to unambiguously obtain the apparent solubility of the gas in the polymer and the associated

change in volume. For this, the Sanchez-Lacombe equation of state was selected to estimate the change in volume of the polymer at different pressures and temperatures [15].

4. THERMOPOROSIMETRY

Since the early work of Thomson [16] it is well established that a fluid confined in the pores of a material exhibits a noticeable shift ΔT of its transition temperature from its liquid to solid state. Furthermore it has been shown that this ΔT-shift is directly related to the sizes of the pores, as expressed by their radius R_p, in which the fluid is trapped [17-19]. Then the knowledge of the R_p (ΔT) function allows the determination of the sizes of the pores of a given material simply by measuring ΔT for a selected fluid [20, 21]. This method, called thermoporosimetry becomes essential for the determination of the pore size distribution in porous materials. The experimental technique which is relatively simple consists in measuring the crystallization temperatures of the fluid confined in the pores and of the ("free") fluid surrounding the material. Actually, the investigated system is made of the porous material over saturated by the fluid and the technique makes use of a sensitive differential scanning calorimeter (DSC). In this context, our original contribution was to use thermoporosimetry to investigate the microstructure of polymeric materials.

Nanoporous sol-gel derived silica monoliths were used to "calibrate" the solvents used for thermoporosimetry. Careful control of the ageing procedure allowed the production of silica gel matrices with tailored textural properties. A number of solvents [22] including linear alkanes, cyclohexane, substituted benzene, CCl_4, acetone, dioxane were tested. Various polymers [23] like polystyrene (PS), ethylene-propylene rubber (EPR), ethylene-propylene-diene-monomer (EPDM), polybutadiene, polyisoprene, poly(dimethyle syloxane) (PDMS), cross linked by UV or gamma irradiation, by heating or ageing degradation, were characterized and their mesh size distributions calculated.

Figure 4 here

To illustrate the use of thermoporosimetry technique we choose the cyclohexane/PDMS system. PDMS sample is a cross linked (by peroxide reaction) and heavily silica loaded one (30% w/w). It is used as a part of an electrical insulator device. Cyclohexane was supplied by

Aldrich and used without further purification. Cyclohexane, as shown by DSC (see Fig.4), exhibits two typical thermal transitions. The cooling from room temperature to –150°C at -0.7°C/min shows two mean exothermal transitions. The first one (at 3.47 °C and releasing 30.38 J/g as specific energy) is the liquid-to-solid normal transition marked by a slight supercooling effect of about 3 °C. The second transition takes place at –88.63 °C and releases 81 J/g namely 2.5 times more than the crystallisation. The latter corresponds to the transition from allotropic phase I to allotropic phase II. It is well established that cyclohexane undergoes conformational transitions between the chair and boat isomeric forms. As indicated by X-ray diffraction the boat isomer proportion is less than 1% at room temperature and smaller at lower temperature [22, 24]. Then the phase I-to-phase II transition cannot be assigned to this conformational change. The signal of the I-to-II transition exhibits two peaks expressing the fact that the observed transition proceeds in two steps. When heating from –150°C to room temperature, the DSC plot shows inverse transitions of those recorded during the cooling. The first one represents the II-to-I transition and occurs at –86.34°C with same specific energy. Unexpectedly, only a single peak is present. At 7.15°C the melting transition occurs releasing 29.6 J/g. When cyclohexane is confined inside a porous material or a swollen polymeric gel, its thermal transition temperatures are consequently shifted; thermoporosimetry uses this temperature shift to calculate the pore or mesh size distributions of these divided media. In this context our contribution, as illustrated in what follows, was to extend the thermoporosimetry in particular towards soft matter characterisation [23, 25].

Figure 5 here

Effectively, based on its two thermal transitions cyclohexane can be used as a thermoporometry probe. Fig.5 shows the DSC exotherms related to confined cyclohexane inside well known textured four different silica gel samples. The characteristics of four silica gels are given in Table 1. According to our calibration procedure [XXX], numerical relationships can be established between the radii of the pores where the cyclohexane undergoes the thermodynamical transitions and the related subsequent temperature depressions. The thermoporosimetry formalism can then be used to calculate the pore or the mesh size distributions (PSD or MSD respectively), namely:

for the liquid to solid transition

$$R_p = 2.02 \exp(-\frac{31.99}{\Delta T}) \quad (6)$$

and for the solid to solid transition

$$R_p = 1.69 + 12.5 \exp(-\frac{1/\Delta T + 0.075}{0.0205}) \quad (7)$$

where R_p is the radius (in nm) of the pore in which the transition takes place and $\Delta T = T_p - T_0$, the depression temperature. T_p being the temperature in pore and T_0 the transition temperature of the bulk cyclohexane (7.15 and –88.63 °C for the solid to solid and for the solid to liquid transitions respectively).

Application to cross linked and filled polymers

PDMS samples of around 10 mg have been left to swell for 48 hours soaking in cyclohexane. A swollen sample was sealed in a DSC aluminum pan and submitted to a cooling temperature program from 10 down to –115 °C with 0.7°C/min ~~temperature~~ rate. Fig. 6 shows the recorded DSC traces. Two groups of exotherms can be pointed out.

Figure 6 here

The first group located at high temperature (between 5 and –20°C) is attributed to the liquid to solid transition (crystallization). In this group the first peak is that of the bulk cyclohexane, the second one is attributed to the confined solvent inside the PDMS macromolecular network. The second group of two peaks appearing at lower temperature represents the solid I to solid II transition undergone by cyclohexane. As expected the first peak is related to the bulk solvent whereas the second one has to be attributed to the trapped cyclohexane. The solid to solid transition, as shown in Figs. 4 and 6, is three times more energetic than the crystallization phenomenon. Peaks of cyclohexane confined in the swollen PDMS sample give a first idea of the mesh size distribution in the polymeric network however, it was demonstrated that the heat of thermal transition is strongly temperature dependent. Without taking in account this dependence, the smallest pore should be underestimated. Following the

calculation procedure described elsewhere [23, 25], the DSC thermograms can be converted to the mesh size distributions. Fig. 7 shows the mesh size distribution MSD of the cross liked silica filled PDMS sample under study. The calculated MSD obtained from the liquid to solid transition is less marked ??? than that derived from the solid to solid one but the satisfactory overlapping of the two distributions has to be noticed. Evidently, the absorbed solvent can be used as a textural probe. Its thermal transitions are highly sensitive to its surrounding constraints. The polymeric meshes of the swollen network limit considerably the degrees of freedom of the cyclohexane molecules macromolecular chains leading to a large depression affecting the phase transition. Thermoporosimetry appears as a unique tool to investigate the cross linked (insoluble) and filled (opaque) polymers.

5. TEMPERATURE MODULATED DIFFERENTIAL SCANNING CALORIMETRY (TMDSC)

The rapid evolution of both methodology and technology has led to recent applications of modulated temperature calorimetry, particularly the combination of the technique with differential scanning calorimetry [26]. Different terms such as « periodic », « oscillating », « dynamic » or « alternating » have thus been used to describe similar techniques based on different types of instruments. The use of temperature modulated DSC to characterize polymers deals mostly with detection of weak transitions, determination of heat capacities in quasi-isothermal mode and separation of superimposed phenomena. The mathematical development necessary to describe the technique is well known [26] and different approaches have been proposed [27]. The total differential heat flow obtained after deconvolution of the modulated heat flow represents the sum of two distinguishable contributions, because the response to the imposed temperature modulation is different depending on the phenomena submitted to the temperature changes. One component, called reversing heat flow, is linked to the heat capacity change; the modifications that depend on the temperature scanning rate can be cycled by alternating heating and cooling effects. The second component is linked to the kinetics and is called non-reversing heat flow, by opposition to the first one; modifications appearing in this signal depend only on the temperature.

The specific heat capacity c_p measured with a conventional DSC, under the conditions of negligible temperature gradient within the sample, is approximately proportional to the temperature difference between the sample and the reference or to the heat flow difference. Calculation of the sample heat capacity is possible through calibration data, at the working temperature, via the following relation (m and m Al_2O_3 are respectively the mass of the sample and the mass of sapphire used as standard calibrating substance) :

$$m c_p = m_{Al_2O_3} c_{p(Al_2O_3)} \frac{a_s - a_b}{a_c - a_b} \tag{8}$$

where the quantities a represent the amplitudes of the heat flow (or temperature) differences signals for different situations corresponding to : sample, calibration and baseline runs designated respectively by 's', 'c' and 'b'. Usually, the baseline run (a_b) is obtained with two empty aluminum pans. In a measuring run (a_s), the sample is in one of the aluminum pans, whereas in the calibration run (a_c) the sample is replaced by the standard sapphire (Al_2O_3), having a well known specific heat capacity. In the case of TMDSC the calibration equation takes the form

$$\left(C_s - C_r\right) = \frac{A_\Delta}{A_{Ts}} \sqrt{\left(\frac{K}{\omega}\right)^2 + C_r^2} \tag{9}$$

where C_S and C_r represent the heat capacities of the sample and of the reference respectively (these quantities include the contribution of the sample and of the pans which can be regarded as identical on the two sides), A_Δ is the temperature difference amplitude between sample and reference, A_{Ts} the sample temperature amplitude (in Kelvin) and ω designates the modulation frequency ($=2\pi/p$ with p being the modulation period in s). K is the temperature-dependent Newton's law constant. When calibrating with sapphire, equation (9) leads to the following equation :

$$\left(C_s - C_r\right) = K_{Cp} \frac{A_{HF}}{\omega\, A_{Ts}} \tag{10}$$

where A_{HF} refers to the amplitude of the differential heat flow, and K_{Cp} is the calibration constant for heat capacity measurements. The heat capacity of the sample obtained using equation (10) allows the determination of the contributions of the reversing and of the non-reversing heat flows respectively, noted HF_{rev} and $HF_{non\text{-}rev}$, to the total heat flow HF_{tot} using the following relations :

HF_{rev} signal = average temperature scanning rate × heat capacity signal (conventionally, on heating a negative sign is necessary because an endothermic effect in the sample, i.e. heat consumption, creates a negative ΔT between the sample and the reference) then, $HF_{non\text{-}rev}$ signal = HF_{tot} signal - HF_{rev} signal

One of the major advantages of the technique described above is most probably the possibility to access directly in a single run to overlapping effects. In this respect, temperature modulated DSC appears to be a more powerful technique than standard DSC. The thermal analyzer used in the present work was a Mettler DSC 821 equipped with a refrigerating cooling system RP 100 (from LabPlant, UK) allowing to work from 200 to 700 K. Taking as an example a polystyrene sample modified by high pressure methane, Fig. 8 illustrates the high potentiality of the technique to detect unambiguously polymer glass transitions. On Fig. 8 the glass transition clearly appears in the HF_{rev} signal, whereas the HF_{tot} signal does not allow detecting the typical inflexion reflecting the glass transition which is hidden in the main fusion peak.

6. CONCLUSION

To modify and characterize polymer microstructures, several techniques relevant to rigorous thermodynamics have been recently developed. Calorimetric techniques, particularly PVT-calorimetry, or scanning transitiometry, and temperature modulated differential scanning calorimetry allow through temperature (or pressure) scans to either modify the polymers micro-organization or to investigate the various transitions undergone by the materials. In addition to the role played by the two variables P and T, a fluid either gaseous (often in supercritical state) or liquid can be advantageously used to promote and/or characterize the

polymer nano/microstructure. A complementary technique which combines a weighing technique and a pressure decay PVT technique allows evaluating the amount of gas penetrating a polymer sample or a porous material during sorption under a precise control of the different parameters.

REFERENCES

1. S.A.E. Boyer, M-H. Klopffer, J. Martin and J-P. E. Grolier. *J. Appl. Pol. Sc*. **103**:1706 (2006).
2. S.L. Randzio, *Pure Appl. Chem*. **63**:1409 (1991).
3. S.L. Randzio, J-P.E. Grolier and J.R. Quint, Rev. *Sci. Instrum*. **65**:960 (1994).
4. S.L. Randzio, J-P.E. Grolier, J. Zaslona and J.R. Quint, French Patent 91-09227, Polish Patent P-295285.
5. S.L. Randzio, Ch. Stachowiak and J-P. E. Grolier. *J. Chem. Thermodyn.* **35**: 639 (2003).
6. S.E.A. Boyer, *Netsu Sokutei* **33** (3):114 (2006).
7. M. Ribeiro, L. Pison and J-P. E. Grolier. *Polymer* **42**:1653 (2001).
8. S.E.A. Boyer, S.L. Randzio and J-P. E. Grolier. *J. Pol. Sc. B. Polym. Phys*. **44**:185 (2006).
9. S. Hilic, PhD Thesis, Blaise Pascal University, France, (2000)
10. S.A.E. Boyer, J-P. E. Grolier, L. Pison, C. Iwamoto, H. Yoshida and T. Iyoda, *J. Therm. Anal. Calorim*. **85**:699 (2006).
11 S.A.E. Boyer, J-P. E. Grolier, H. Yoshida and T. Iyoda, *J. Pol. Sc. B. Polym. Phys*. **45**:1354 (2007).
12. L. Coiffard, J-P. E. Grolier, V. Eroshenko. *AIChE J., 2005,* **51**:, 1246-*1257*

13. S. Hilic, A.A.H. Padua, J-P.E. Grolier. *Rev. Sci. Instrum*., **71**: 4236 (2000).
14. S. Hilic, S.A.E Boyer, A.A.H. Padua, J-P.E. Grolier. *J. Polym. Sci. B : Polym. Phys.*, **39**: 2063 (2001).
15. S.A.E. Boyer, J-P.E. Grolier. *Polymer* **46**: 3737 (2005).
16. W. Thomson. *Phil. Mag*. **42**: 448 (1871).
17. W.A. Patrick and W.A. Kemper, *J. Phys. Chem*., **42**:369 (1937).
18. C.L. Jackson, G.B. McKenna. *J. Chem. Phys*., **93**:9002 (1990).
19. C.L. Jackson, G.B. McKenna. *Rubber Chem. Technol*., **64**:760 (1991).
20. M. Brun, A. Lallemand, J.-F. Quinson and C. Eyraud. *Thermochim. Acta* **21**: 59 (1977).
21. N. Billamboz, M. Baba, M. Grivet and J.-M. Nedelec. *J. Phys. Chem. B*., **108**:12032 (2004).
22. G.J. Kabo, A.A. Kozyro, M. Frenkel and A.V. Blokhin. *Mol. Cryst. Liq. Cryst*., **326**: 333 (1999).
23. N. Billamboz, J.-M. Nedelec, M. Grivet and M. Baba. *ChemPhysChem*., **6**:1 (2005).
24. Y. Shao, G. Hoang and T.W. Zerda. *J.Non-Cryst. Solids*, **182**: 309 (1995).
25. N. Bahloul, M. Baba, and J-M. Nedelec. *J. Phys. Chem. B ~~Letters~~* **109**: 16227 (2005).
26. M. Reading, D. Elliot, V.L. Hill. *J. Therm. Anal*. **40**:949 (1993).

27. J.E.K. Schawe. *Thermochim. Acta* **261**:183 (1995).

Figure Captions

Figure 1. Schematic view of PVT-controlled scanning calorimetry showing two main scanning situations, the Pressure-controlled scanning calorimetry (PCSC) situation and the Temperature-controlled scanning calorimetry (TCSC) situation. The PCSC situation, under isothermal P-scans, yields through the thermal output the isobaric thermal expansivity (here $\alpha_{pol\text{-}g\text{-}int}$ is for a polymer sample interacting with a gas). The TCSC situation, under isobaric T-scans, yields through combination of both thermal and mechanical outputs the entropy change.

Figure 2. Schematic representation of PVT-controlled scanning calorimetry showing the calorimetric detector housing the twin cells connected to the high-pressure PVT line. According to the respective role of the measuring M and reference R cells, three thermal modes are described. In PCSC situation: a, the thermal differential comparative mode, where both measuring and reference cells contain a polymer and are connected to the gas line; b. thermal differential mode, where the measuring cell contains the polymer and the reference cell contains an inert sample of equal volume, both cells are connected to the gas line. In TCSC situation: c, the simple thermal differential mode, where the measuring cell contains the polymer and is connected to the gas line while the reference cell acts as a thermal reference.

Figure 3. Schematic picture showing the liquid crystal $PMA(Az)_n$ domain surrounding the PEO_m nanoscaled cylinders in the smectic phase; the PEO_m domain can expand under super critical CO_2 sorption.

Figure 4. Thermal transitions of bulk cyclohexane observed under 0.7°C/min scanning rate.

Figure 5. DSC curves of cyclohexane. The endotherms are related to the bulk cyclohexane whereas the exotherm signals represent the thermal transitions (liquid to solid I at higher temperatures and solid I to solid II at lower ones) of the confined solvent. R1 to R4 are the silica gel samples calibration described in Table 1. The scanning rate is 0.7°C/min.

Figure 6. DSC traces obtained in the case of cyclohexane swelling a PDMS sample. The scanning rate is of 0.7°C/min.

Figure 7. Mesh size distribution (MSD) of a cross linked silica loaded PDMS sample swollen by cyclohexane, calculated either from the liquid to solid transition or from the solid to solid transition respectively.

Figure 8. Thermograms obtained with temperature modulated differential calorimetry for a polystyrene sample modified by sorption of methane under high pressure (150 MPa). The reversing heat flux HF_{rev} shows clearly the glass-transition inflexion curve which is otherwise hidden in the main fusion peak of the total heat flux HF_{tot}.

Table 1. Textural characteristics of samples used for calibration: SSA, the specific surface area; V_p, the porous volume; σ, the uncertainty on V_p; R_p, the pore radius; MaxPSD, the maximum of the pore size distribution.

Sample	*SSA* (m^2/g)	*Vp* (cm^3/g)	*Rp* (Å)	*Max PSD* (Å)
R4	532	0.696	26.2	24
R3	473	0.922	39	34.2
R2	166	0.991	119.2	87
R1	183	1.327	144.9	142.5

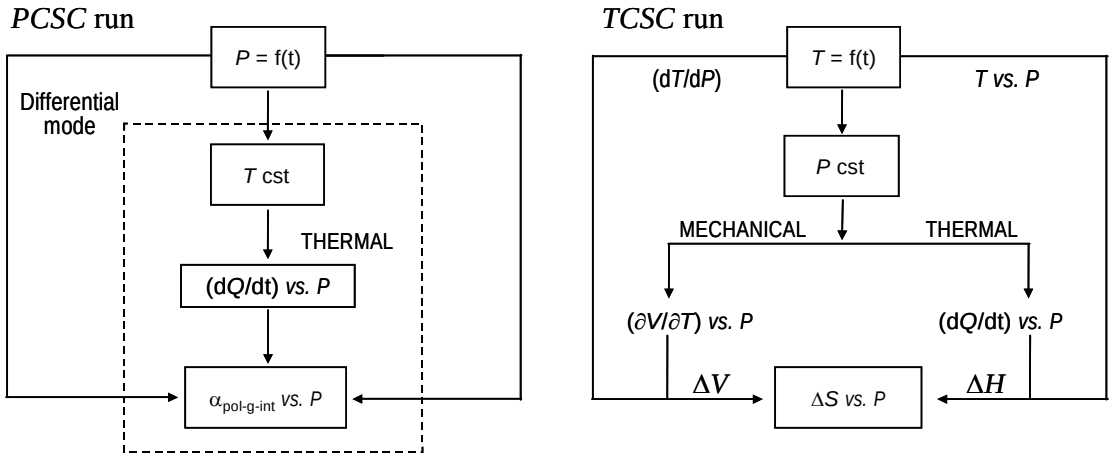
PCSC run
P = f(t)
Differential mode
T cst
THERMAL
(dQ/dt) vs. P
αpol-g-int vs. P
TCSC run
T = f(t)
(dT/dP)
T vs. P
P cst
MECHANICAL
THERMAL
(∂V/∂T) vs. P
(dQ/dt) vs. P
ΔV
ΔS vs. P
ΔH

Figure 1

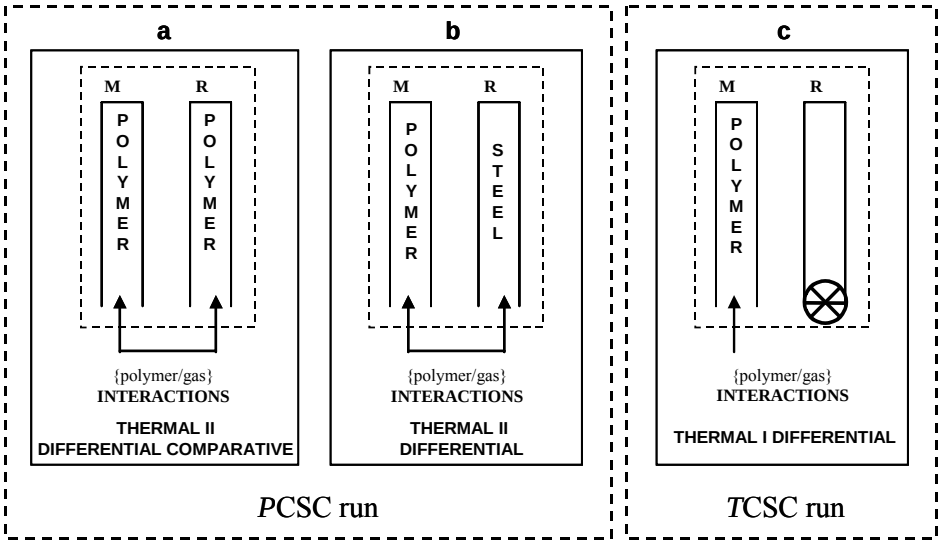
a
b
c
M
R
POLYMER
POLYMER
POLYMER
STEEL
POLYMER
{polymer/gas}
INTERACTIONS
{polymer/gas}
INTERACTIONS
{polymer/gas}
INTERACTIONS
THERMAL II
DIFFERENTIAL COMPARATIVE
THERMAL II
DIFFERENTIAL
THERMAL I DIFFERENTIAL
PCSC run
TCSC run

Figure 2

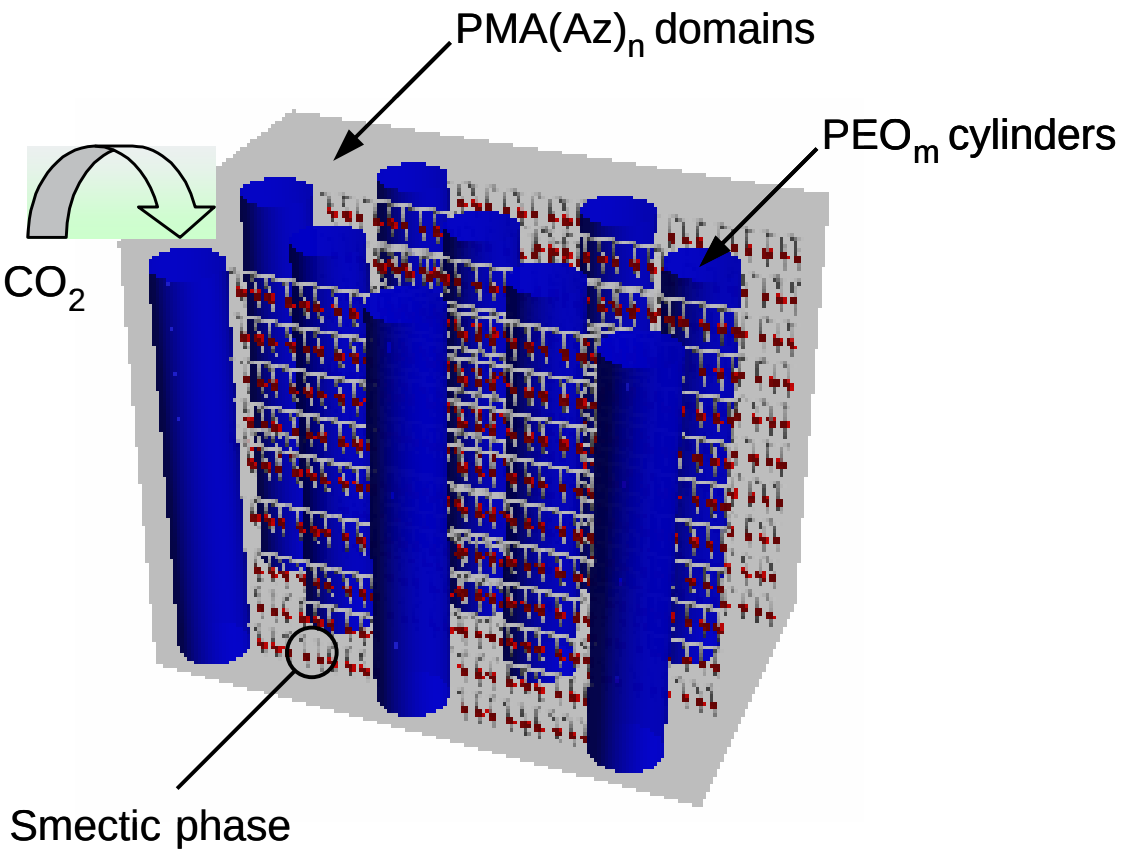

Figure 3

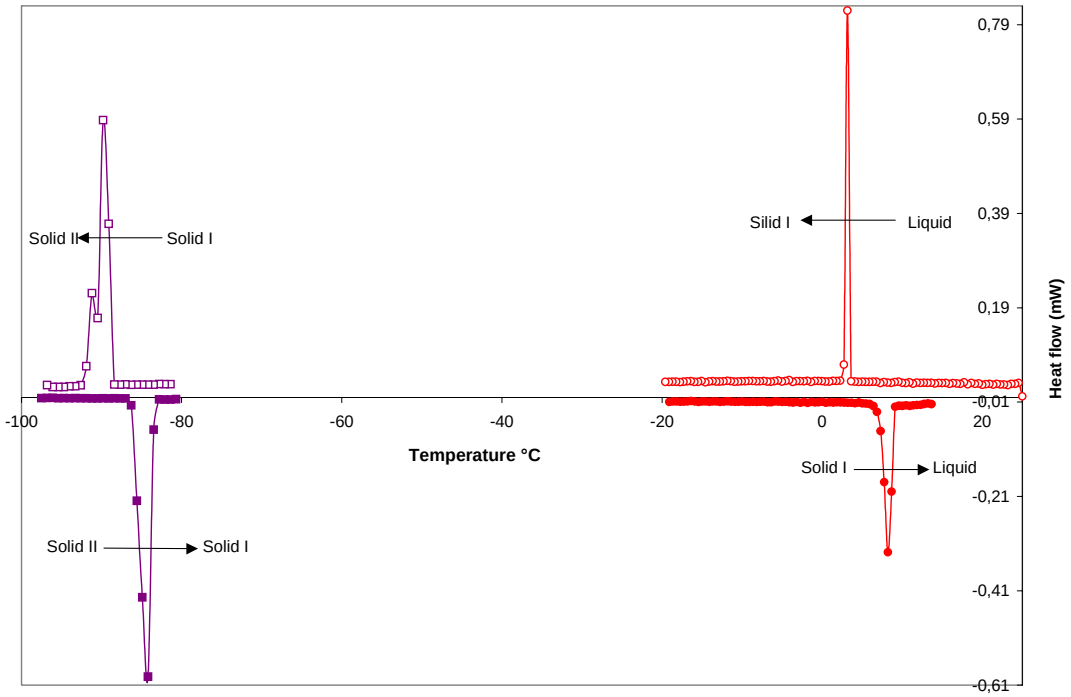
0,79
0,59
0,39
0,19
-0,01
-0,21
-0,41
-0,61
Heat flow (mW)
-100
-80
-60
-40
-20
0
20
Temperature °C
Solid II
Solid I
Silid I
Liquid
Solid I
Liquid
Solid II
Solid I

Figure 4

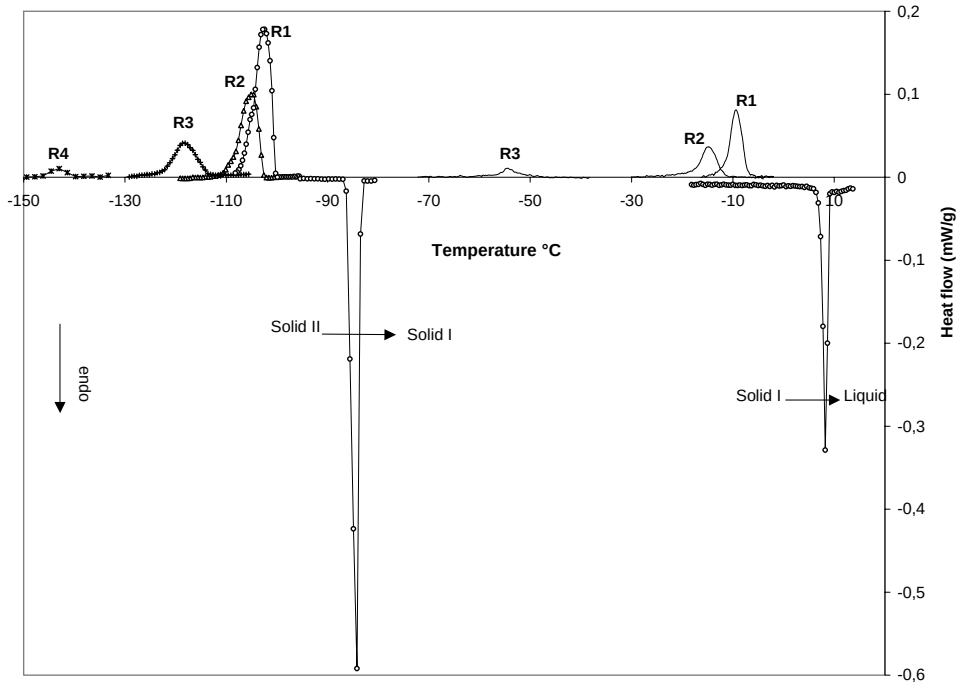
R1
R2
R3
R4
R3
R2
R1
0,2
0,1
0
-0,1
-0,2
-0,3
-0,4
-0,5
-0,6
-150
-130
-110
-90
-70
-50
-30
-10
10
Temperature °C
Heat flow (mW/g)
Solid II
Solid I
Solid I
Liquid
endo

Figure 5

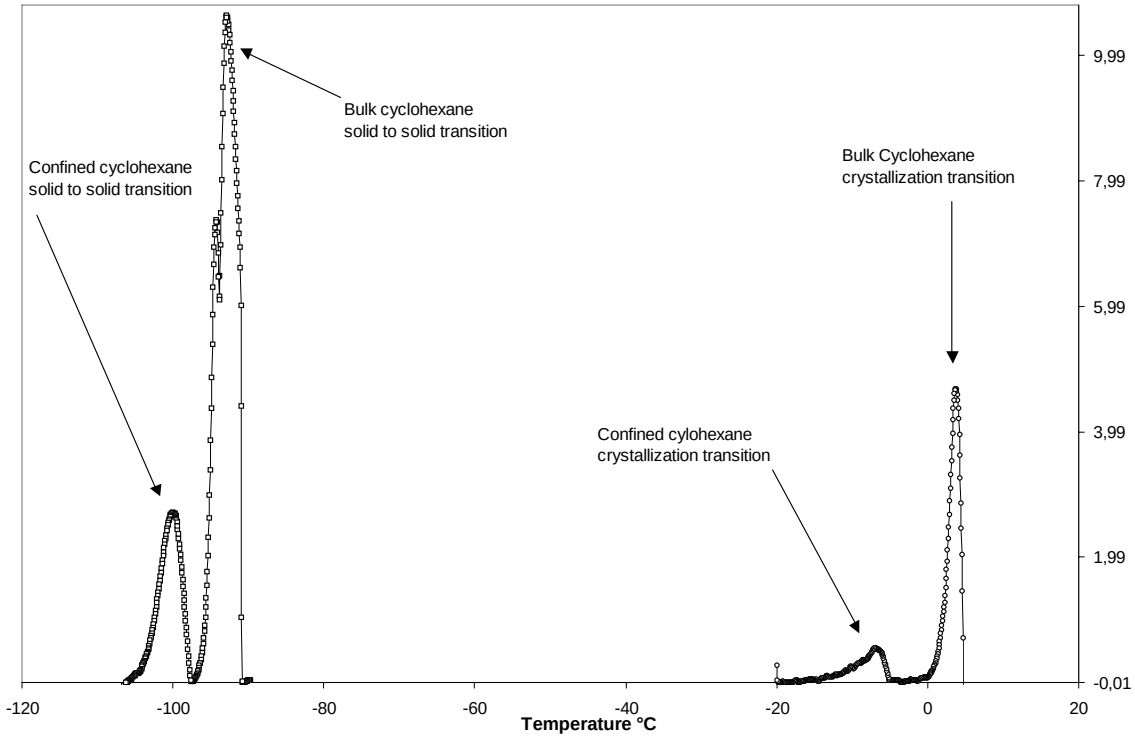
Confined cyclohexane
solid to solid transition
Bulk cyclohexane
solid to solid transition
Bulk Cyclohexane
crystallization transition
Confined cylohexane
crystallization transition
9,99
7,99
5,99
3,99
1,99
-0,01
-120
-100
-80
-60
-40
-20
0
20
Temperature °C

Figure 6

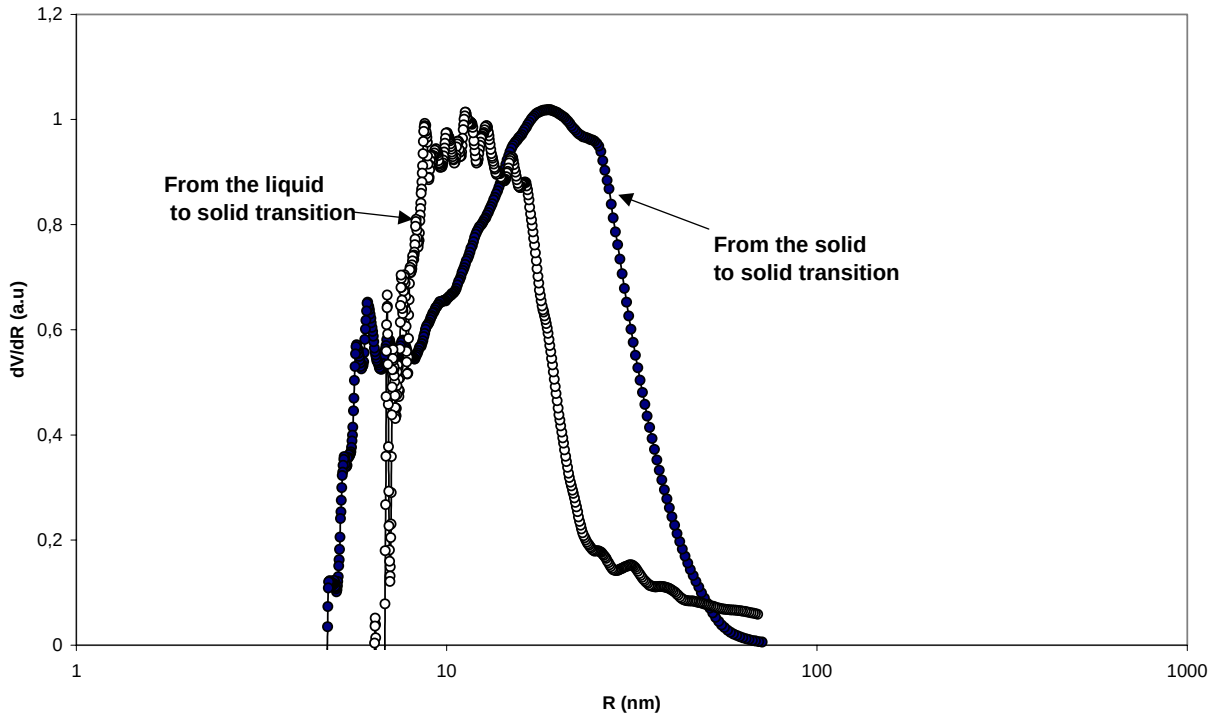
1,2
1
0,8
0,6
0,4
0,2
0
dV/dR (a.u)
From the liquid
to solid transition
From the solid
to solid transition
1
10
100
1000
R (nm)

Figure 7

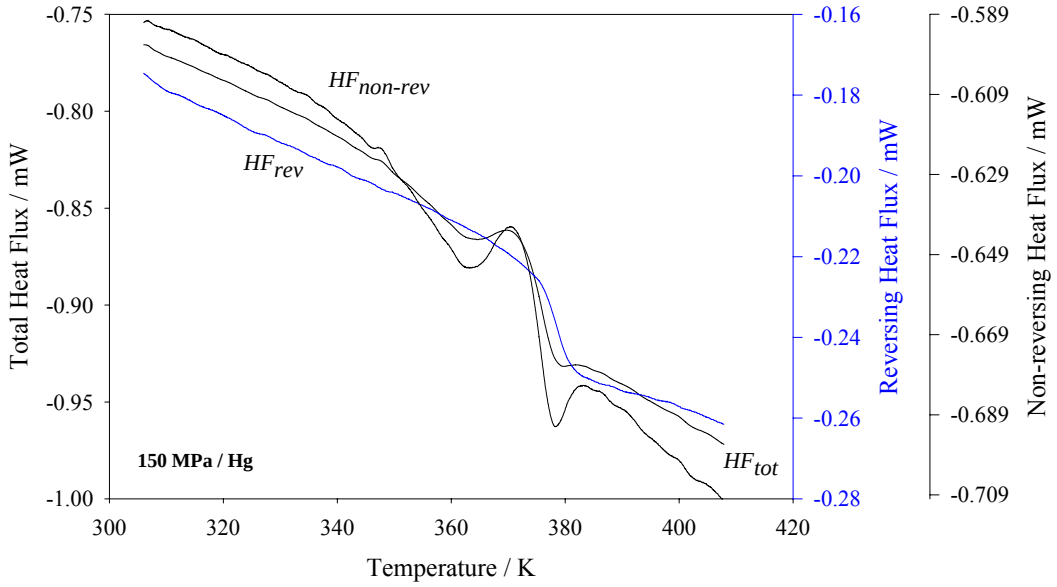
-0.75
-0.80
-0.85
-0.90
-0.95
-1.00
Total Heat Flux / mW
-0.16
-0.18
-0.20
-0.22
-0.24
-0.26
-0.28
Reversing Heat Flux / mW
-0.589
-0.609
-0.629
-0.649
-0.669
-0.689
-0.709
Non-reversing Heat Flux / mW
300
320
340
360
380
400
420
Temperature / K
HF non-rev
HF rev
HF tot
150 MPa / Hg

Figure 8